Conformation of a Protein Kinase C Substrate, NG(28–43), and Its Analog in Aqueous and Sodium Dodecyl Sulfate Micell Solutions

Ding-Kwo Chang, Wei-Jyun Chien, and A. I. Arunkumar
Institute of Chemistry, Academia Sinica, Taipei, Taiwan, Republic of China

ABSTRACT A peptide corresponding to the neuronal protein neurogranin (NG) residues 28–43, NG(28–43), and its analog, [A^{35}]NG(28–43), have been investigated by NMR, electron paramagnetic resonance (EPR), and circular dichroism (CD) spectroscopies. The peptides existed in aqueous solution predominantly in random form. However, a nascent helical structure was detected in the central region of the parent peptide from NMR data. Furthermore, a helical structure can be detected for both peptides with greater induced secondary structure for the parent peptide in the presence of sodium dodecyl sulfate (SDS) micelle. The formation of micelles for SDS was confirmed by results from EPR as well as ^{13}C NMR. As shown by CD experiments, helical conformer was induced for NG(28–43) in vesicular solution containing phosphatidyl serine (PS), whereas no helix can be discerned for the peptide in phosphatidyl choline (PC)-containing vesicular solution. Together with the induction of the peptide into helix in SDS micellar solution as suggested by both NMR and CD data, these results underscored the electrostatic contribution to the interaction of the PKC substrate peptides and proteins with membrane. According to NMR and CD data, a dynamic equilibrium existed between free and micelle-bound states for the peptide. Moreover, proton-deuterium exchange results and SDS-induced linewidth broadening of proton resonances allowed delineation of the orientation of the amphipathic helix on the surface of SDS micelle. The result was supported by spin label experiments that indicated F35 of NG(28–43) interacted strongly with the hydrocarbon interior of micelle. Based on the experimental findings, a working model was proposed that attempted to partly explain the roles played by the nonpolar amino acid near the phosphorylation site, by the negatively charged phospholipids, and by the basic amino acids of the substrate.

INTRODUCTION

Protein kinase C (PKC) has been shown to play important roles in controlling a variety of physiological processes, including tumor promotion, signal transduction, exocytosis, gene expression, and long-term potentiation (Nishizuka, 1988; Huang, 1989). It was found in different tissues as multiple isoforms (Huang et al., 1986; Huang et al., 1987; Koide et al., 1992; Ogita et al., 1992). PKC is a phospholipid-dependent, calcium-activated kinase that phosphorylates highly selective substrate proteins at either Ser or Thr. Among the phospholipid cofactors, the negatively charged phosphatidyl serine (PS), the major acidic lipid in the inner leaflet of mammalian plasma membranes (Devaux, 1992), is most commonly used for PKC studies. Recently, two brain-specific PKC-selective substrates, neuromodulin and neurogranin, have been reported (Baudier et al., 1989; Dekker et al., 1989). Neuromodulin has been shown to be involved in nerve growth and neuroplasticity (Meiri et al., 1988; Nelson et al., 1989; Represa et al., 1990; Watson et al., 1990), whereas neurogranin appears to be related to long-term potentiation of the hippocampus (Klann et al., 1992). Both have been shown to be phosphorylated by PKC in intact cells in hippocampal slices (Baudier et al., 1991; Gianotti et al., 1992). They bear a high degree of sequence homology in the domain encompassing the phosphorylation site. The domain is absolutely conserved in all fish and mammalian neuromodulin sequences known, suggesting its essential functional role.

Requirements for the selective substrate of PKC include basic amino acids on both sides of the phosphorylation site (Ser/Thr) as well as a Phe or hydrophobic amino acid immediately adjacent to the site (Gianotti et al., 1992; Aderem, 1992; Pearson and Kemp, 1991). An interesting study by Davis et al. on phosphorylation of the transferrin receptor by PKC demonstrated that Ser24, which is followed by Leu but not Ser63, which is not adjacent to a hydrophobic residue, was phosphorylated by PKC (Davis et al., 1986). The data highlighted the critical role assumed by the hydrophobic residue immediately C-terminal to the phosphorylation site. A high concentration of clustered basic amino acids appears to be necessary to compensate the effect of deleting the hydrophobic residue in the neighborhood of a phosphorylation site (Pearson and Kemp, 1991). In studies of the latter determinant, a decrease of more than three orders of magnitude in phosphorylation efficiency was reported as Ala was used to substitute for Phe in the synthetic peptide homologous to the region surrounding a phosphorylation site, in the presence of vesicles formed by the lipid cofactors PS and diacylglycerol (DAG) (Chen et al., 1993).

A close correlation has been demonstrated between association of the PKC substrate proteins with membrane and their phosphorylation by PKC (Bazzi and Nelsestuen, 1987; Edashige et al., 1992). The region surrounding the phosphorylation site appears to be exposed in the whole sub-

Received for publication 18 March 1996 and in final form 11 November 1996.

Address reprint requests to Dr. Ding-Kwo Chang, Institute of Chemistry, Academica Sinica, Taipei, Taiwan 11529, Republic of China. Tel.: 886-2-789-8594; Fax: 886-2-783-1237; E-mail: dkc@chem.sinica.edu.tw.

0006-3495/97/02/554/13 $2.00

strate protein (consisting of 78 amino aicds for bovine neurogranin) as a monoclonal antibody, NM2 was found to recognize the PKC phosphorylation site with the suggested epitope QASFR (Oestreicher et al., 1994). Thus the segment surrounding the phosphorylation site is likely to interact with the membrane before approaching PKC on the surface of membrane. Moreover, because of the hydrophilic nature of both proteins, their association with the membrane is expected to be extrinsic (Houbre et al., 1991; Skene and Virág, 1989), as also verified by the linewidth measurement of backbone NH resonance peaks in sodium dodecyl sulfate (SDS) solution in the present study. The membrane-bound substrate would be presented to the active site of membrane-bound PKC by reorientation and probably by diffusion (Houbre et al., 1991). Because it is likely that the substrates of PKC are phosphorylated only in the proximity of membrane (Bazzi and Nelsestuen, 1987) and because negatively charged PS is essential for activation of many PKC isozymes (Kaibuchi et al., 1981; Mahoney and Huang, 1995), SDS was employed as a model for the membrane formed by phospholipids.

To investigate the structural basis for the role of highly conserved hydrophobic residue C-terminal to the phosphorylation site and for the dramatic difference in the kinetic behavior between the wild-type and mutant peptides observed by Chen et al. (1993), circular dichroism (CD), NMR, and electron paramagnetic resonance (EPR) spectroscopies were initiated. The conformation is determined by distance geometry and simulated annealing employing distance and dihedral angle constraints derived from NMR data. The association of the peptide with micelles was probed by EPR and NMR lineshape analyses. It was found from CD and NMR results that the peptide corresponding to residues 28–43 of a bovine neurogranin underwent conformational change as SDS micelles or vesicles containing PS were introduced into aqueous solution. Specifically, α-helix is induced for the peptide at the expense of random coil by association with SDS micelles and with vesicles containing PS. The hydrophobic side of the induced helix is shown to associate with the interior of the micelle from EPR and NMR linewidth results. The long-range electrostatic force is assumed to be responsible for anchoring the substrates on the surface of the membrane, expediting their encounter with PKC. The role played by the Phe residue C-terminal to the phosphorylation site is discussed in the context of interaction between the PKC substrate and the hydrophobic interior of the membrane. Coupled with the stability of the helix of the parent peptide, this specific interaction may partially account for the three orders of magnitude decrease in the phosphorylation kinetics for its A35 analog.

MATERIALS AND METHODS

Peptide synthesis

Peptides were synthesized in an automatic mode by a solid-phase sythesizer (model 431A; Applied Biosystems, Foster City, CA) using 9-fluorenylmethoxycarbonyl chemistry. The peptides were cleaved from the resin and simultaneously deprotected using a mixture of trifluroacetic acid/phenol/thioanisole/ethanedithiol in distilled water (84:6:4:4:2, v/v) for 2 h at 277 K, and the crude peptides were subsequently purified by reverse-phase high-performance liquid chromatography on a C_{18} column with acetonitrile gradients in aqueous solution containing trifluoroacetic acid. The primary sequence of the peptides was ascertained by amino acid analysis as well as electrospray mass spectrometry.

1,2-Dihexadecanoyl-sn-glycero-3-phosphocholine (PC), 1,2-dihexadecanoyl-sn-glycero-3-phospho-L-serine (PS), and 1,2-dihexadecanoyl-sn-glycerol (DAG) were purchased from Sigma (St. Louis, MO). SDS-d_{25} was purchased from CIL (Andover, MA)

CD spectropolarimetry

All of the CD experiments were carried out on a Jasco 720 spectropolarimeter at 298 K. The spectra were recorded from 190 to 270 nm at a scanning rate of 20 nm/min with a time constant of 2 s. Spectra were obtained from an average of five scans with a step resolution of 5 nm and a bandwidth of 1 nm at 298 K, using cells with a path length between 1 and 5 mm.

For estimation of the secondary structure content, the observed ellipticity was converted into mean residue ellipticity (deg·cm·dmol^{-1}), using the relationship $[\theta] = \theta \cdot l^{-1}c^{-1}N^{-1}$, where θ is measured ellipticity, l is the path length in centimeters, c is the molar concentration of the peptide, and N is the number of amino acids in the peptide sequence. Percentage helicity was calculated (Scholtz et al., 1991) using $[\theta]$ at 222 nm according to $100\,[\theta]_{222}/[\theta]_{max}$, where $[\theta]_{max} = -40{,}000[1 - (2.5/N)]$, $N = 16$ in the present study.

Preparation of SDS micelles, PS, PS/DAG, and PC vesicles

The micelles and vesicles were prepared by mixing SDS or the phospholipids with appropriate amounts of peptides and/or spin label. The mixtures were incubated in a bath at 298 K and sonicated for at least 2 h. For CD experiments, peptide concentrations were between 15 and 75 μ M, whereas 0.03 to 2 mM of each of the phospholipids was used for vesicular solutions. Tha pH of the sample solutions was adjusted to 7.0 by phosphate buffer.

EPR spectroscopy

The spin label reagent, 12-doxyl stearic acid methyl ester (12-SASL), purchased from Sigma, was used in the experiments without further purification. The EPR spectra were acquired on a Bruker ESP 300 continuous-wave spectrometer with samples containing 0.4 mM of the spin label and SDS ranging from 0 to 100 mM in concentration. X-band, first-derivative absorption EPR spectra were obtained at 298 K with the following parameters: modulation 1 G at 100 kHz, microwave power 1 mW, and total sweep width 80 G.

The observed proton resonance line broadening arises primarily from the dipolar interaction between the unpaired electron and the proton.

NMR spectroscopy

The peptide samples were prepared in 90% H_2O/10% D_2O and in 55 mM deuterated SDS micelles/90% H_2O/10% D_2O to a concentration of 2.2 mM peptide at pH 6.1. For deuterium-proton exchange experiments, samples were prepared in either 100% D_2O, or 55 mM SDS-d_{25}/100% D_2O at pH 3.0. The samples were maintained at the desired pH in 10 mM phosphate buffer.

The ^{1}H NMR spectra were acquired on a Bruker AMX-500 spectrometer with a spectral width of 5000 Hz. The TPPI method (Marion and Wüthrich, 1983) was used for the absorption-mode NOESY experiments with mixing times of 100 and 250 ms, whereas the MLEV-17 spin-lock

pulse sequence was utilized in TOCSY experiments (Braunschweiler and Ernst, 1983) with mixing times of 60 and 100 ms. In addition, DQF-COSY experiments (Rance et al., 1983) were employed for coupling constant measurements. Generally, 384–512 t_1 increments were used with 64–96 FID transients in 2K data points (8K for DQF-COSY sepctra). Suppression of HOD solvent signal was achieved by soft presaturation or the jump-return or WATERGATE (Piotto et al., 1992) method. Data were processed using the Bruker processing program UXNMR and Felix interfaced to Biosym software programs (Biosym, Inc., San Diego, USA). A 45 or 60 shifted sine-bell window function was applied to FIDs in each dimension before Fourier transformation and the data were zero filled to $2k \times 1k$ ($8k \times 1k$ for DQF-COSY) data points. All chemical shifts were referenced externally to the methyl resonance of 4,4-dimethyl-4-silapentane-5-sulfonic acid (DSS; 0 ppm). The Karplus equation was used to estimate the backbone dihedral angle ϕ (Karplus, 1959).

NOE intensity is proportional to the inverse sixth power of interproton distance (Ernst et al., 1987). The data were converted into interproton distance using methylene protons of histidine or the 2H and 3H of the phenyl ring of phenylalanine as a reference. Depending on the distance, 0.6 to 1.0 Å was allowed to vary for the distance restraints in the structure computation.

Proton-deuterium exchange experiments were carried out by adding D_2O to the lyophilized peptide sample or peptide/SDS mixture. The temperature for the experiments in SDS-free solution was set at 278 K, whereas for those in SDS micelle solution, the temperature was raised to 288 K, because at lower temperatures SDS aggregated. A TOCSY experiment was performed for SDS-containing solution to ascertain the peak assignment.

^{13}C NMR spectra were acquired at 298 K on the same spectrometer operating at 125.76 MHz to monitor the SDS micelle formation and location of the spin label in the micelle. 1024 FID transients were collected, with a recycle delay of 2 s for all of the experiments.

Structure computation

A total of 210 NMR-derived constraints (including 14 torsional constraints) were used in structure computation using distance geometry/simulated annealing (DG/SA) methods (Nilges et al., 1988) implemented in the Biosym NMRchitect programs (version 2.3). A final family of 20 structures was generated that are compatible with the NMR-derived constraints. Leonard-Jones 6–12 van der Waals energy was replaced by a quadratic term in the initial stages of the simulated annealing run. In the process of simulated annealing, the temperature was increased to 1000 K for a molecular dynamics run of 5 ps to allow more conformational space to be explored. The system was cooled down to 300 K in seven steps (for 20 ps) and minimized by steepest descent and conjugated gradient methods before final structures were obtained.

RESULTS AND DISCUSSION

EPR spectra of the spin label in the absence and in the presence of various concentrations of SDS and $NG_{(28-43)}$ are presented in Fig. 1, *A–D*. Compared with Fig. 1 *A*, the lineshape changes significantly in the presence of more than 20 mM SDS (Fig. 1, *C* and *D*), which is in the concentration range used in the NMR experiments. The rotational correlation times (τ_r) calculated from Fig. 1, *A*, *B*, *C*, and *D*, are, respectively, 0.57×10^{-10}, 8.6×10^{-10}, 8.0×10^{-10}, and 7.7×10^{-10} s (Stone et al., 1965; Cannon et al., 1975). These results show that an increase of more than one order of magnitude in τ_r occurs as the spin label associates with SDS, suggesting the formation of micelles for SDS (Brown et al., 1981). This conclusion is in agreement with the reported critical micelle concentration (cmc) of 8 mM for

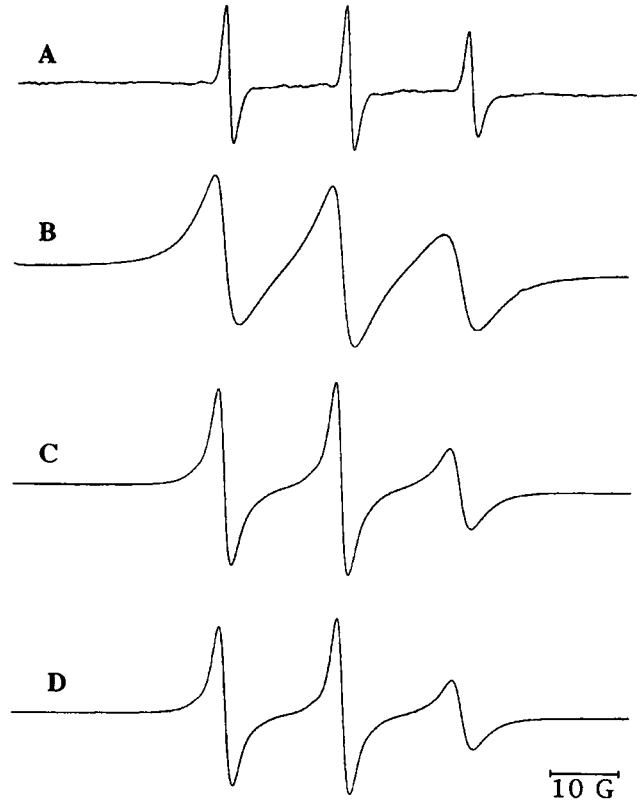

FIGURE 1 X-band EPR spectra of 0.4 mM 12-SASL as a function of the concentration of SDS. The spectra were measured at 298 K for an SDS concentration of (*A*) 0 mM, (*B*) 20 mM, and (*C*) 50 mM. In *D*, the spectrum was obtained from a solution containing 0.4 mM 12-SASL, 100 mM SDS, and 0.2 mM $NG_{(28-43)}$. Concentrations of SDS in *B–D* are above cmc for SDS, and the micelle formation is supported by comparison of calculated rotational correlation times from *A* and from *B* through *D*.

SDS (Mysels and Prinzen, 1959). The τ_r value calculated from Fig. 1 *D* is essentially the same as those obtained from Fig. 1, *B* and *C*, indicating that the size of the micelle is not altered by interaction with the peptide $NG_{(28-43)}$.

The fingerprint and NH-NH regions of NOESY spectrum for $NG_{(28-43)}$ peptide in SDS solution are displayed in Fig. 2. The sequential connectivity can be clearly discerned, because of sufficiently dispersive resonance peaks. The strong, abundant $d_{NN}(i, i + 1)$ NOE cross-peaks indicate a well-defined, folded structure for the wild-type hexadecameric peptide in SDS micelle solution. Representative non-sequential NOE peaks, particularly $d_{\alpha\beta}(i, i + 3)$ peaks, are shown in Fig. 3. These peaks and strong $d_{NN}(i, i + 1)$ peaks shown in Fig. 2 *B* are characteristics of an α-helix (Wüthrich, 1986). NOE interactions among side-chain protons are displayed in Fig. 4 for $NG_{(28-43)}$ in SDS micelle solution. The moderately strong medium-range NOE peaks are also a manifestation of an α-helical structure for the wild-type peptide in SDS solution. Table 1 lists the chemical shift of ^1H resonance peaks of $NG_{(28-43)}$ in 90% H_2O/10% D_2O and in SDS micelle solutions at 298 K.

A less ordered structure for the parent peptide in the SDS-free solution than in the SDS-containing solution is

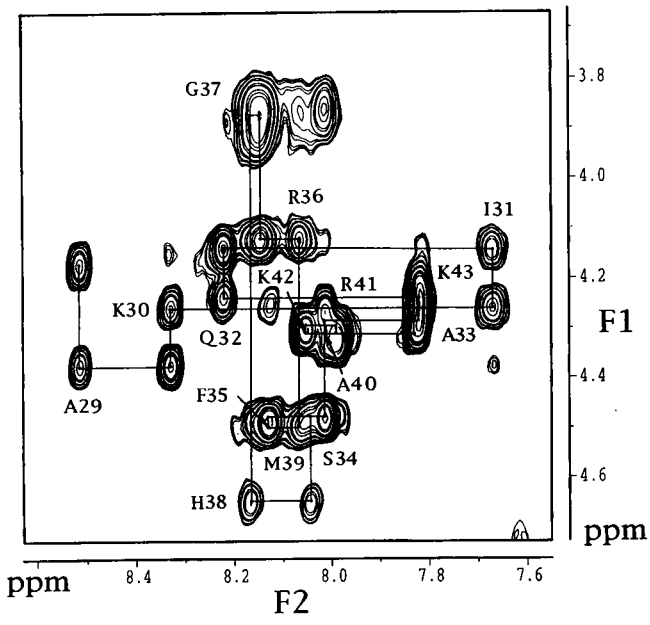

FIGURE 2 NH-αH region of the NOESY spectrum at a mixing time of 250 ms for 2.2 mM $NG_{(28-43)}$ in 55 mM SDS-d_{25} solution at 298 K and pH 6.1, showing sequential connectivities.

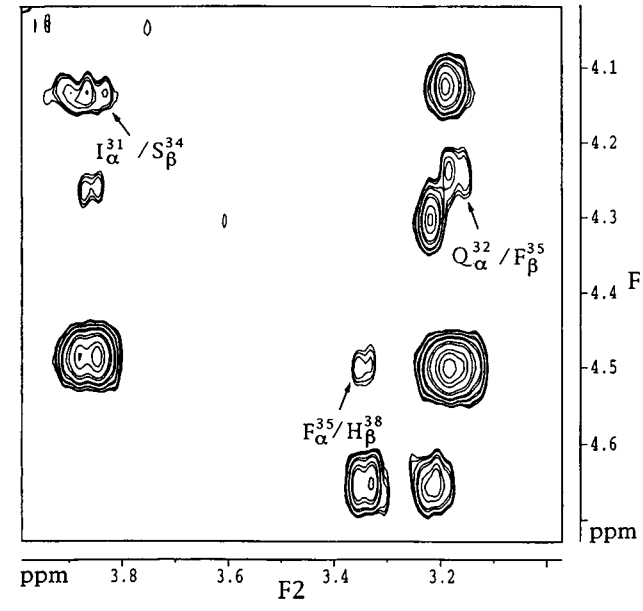

FIGURE 4 Portion of the NOESY spectrum at a mixing time of 250 ms for 2.2 mM $NG_{(28-43)}$ in 55 mM SDS-d_{25} at 298 K and pH 6.1.

suggested by considerably fewer and weaker observable NOE cross-peaks in the SDS-free aqueous solution. The only exceptions are the peaks involving G37, whose amide proton resonates at a relatively high field and has several (i, i + 2)-type NOE interactions for the parent peptide in aqueous solution. These observations are consistent with the notion that a nascent helical structure exists in the $NG_{(28-43)}$ peptide surrounding G37 (Dyson et al., 1988). In contrast, much weaker nonsequential NOE peaks are found for the segment encompassing G37 of $[A^{35}]NG_{(28-43)}$ analog. Furthermore, in aqueous solution the resonance signal for NH of G37 of $NG_{(28-43)}$ is 0.46 ppm upfield relative to that of G37 in $[A^{35}]$ analog at δ 8.32 ppm. As inferred from NOE patterns, $[A35]NG_{(28-43)}$ adopts random coil conformation in the region surrounding G37, so that G37 of the parent peptide cannot be part of random structure, but is part of a folded structure such as a turn or helix. This is because the chemical shift of amide proton in an α-helix is upfield relative to that of random coil (Wishart et al., 1991). Alternatively, the upfield shift of the NH of G37 could arise from the ring current effect of the side chain of F35 (Jackman and Sternhell, 1969) in a rigid turn structure. These results suggest that the wild-type peptide forms a folded structure in the region F35-G37 and has a greater tendency to form a helix. In conformity with NMR data, analysis of the two peptides using the secondary structure prediction algorithm proposed by Ptitsyn and Finkelstein (1983) shows a higher probability that the parent peptide will form an α-helix, both in water and in membranous environments.

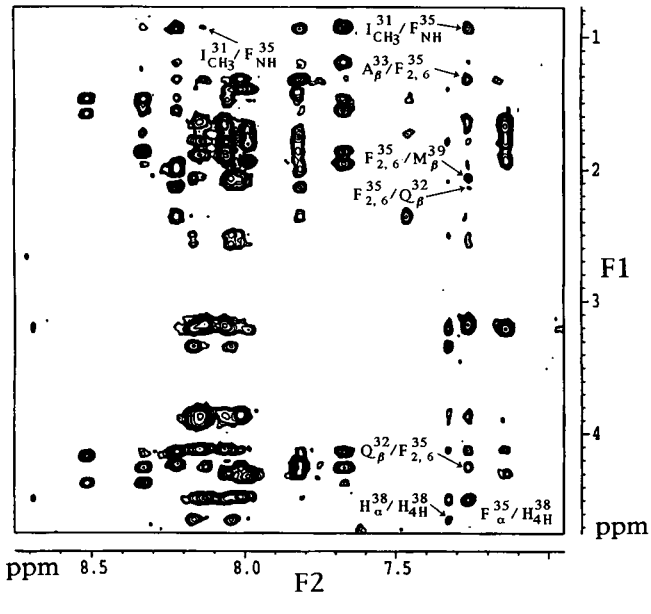

FIGURE 3 Representative $d_{\alpha\beta}(i, i + 3)$ NOE interactions from the same NOESY spectrum as in Fig. 2.

NOE peaks detected for $NG_{(28-43)}$ and for $[A^{35}]NG_{(28-43)}$ in water and in SDS micelle solutions are summarized in Fig. 5. It is of interest to observe that the glycine residue of $NG_{(28-43)}$ is in the middle of a helical structure in the micellar environment, in contrast to the common observation that glycine is a helix terminator in aqueous solution (Richardson and Richardson, 1989). Results of the proton-deuterium exchange experiments for $NG_{(28-43)}$ at 288 K in SDS micelle solution are displayed in Fig. 6. The NH spectra at the bottom, middle, and top of the figure are data taken immediately, 20 min, and 5 h, respectively, after the addition of D_2O to the lyophilized peptide/SDS mixture. The backbone amide protons of residues I31, F35, M39, and

TABLE 1 ^{1}H NMR chemical shifts (ppm) of $NG_{(28-43)}$ at pH 6.1, 298 K in 90% H_2O/10% D_2O and in 55 mM SDS-d_{25}

Residue	NH	αH	βH		Others
Ala28		4.09	1.52		
		4.18	*1.57*		
Ala29	8.59	4.32	1.37		
	8.51	*4.38*	*1.46*		
Lys30	8.45	4.28	1.83	1.67	γCH$_2$ 1.43; δCH$_2$ 1.74
	8.32	*4.26*	*1.85*	*1.72*	*1.42* *1.53*
					εCH$_2$ 2.99; εNH$_3^+$ 7.53
					3.02 *7.45*
Ile31	8.26	4.13	1.81		γCH$_2$ 1.46 1.17
	7.66	*4.14*	*1.95*		*1.55* *1.18*
					γCH$_3$ 0.87; δCH$_3$ 0.83
					0.93 *0.91*
Gln32	8.53	4.31	2.07	1.95	γCH$_2$ 2.34; δNH$_2$ 7.54 6.87
	8.22	*4.23*	*2.12*	*2.01*	*2.36* *7.46* *6.76*
Ala33	8.43	4.27	1.34		
	7.81	*4.27*	*1.32*		
Ser34	8.25	4.38	3.80	3.80	
	8.01	*4.48*	*3.88*	*3.84*	
Phe35	8.28	4.62	3.09		2,6H 7.33; 3,5H 7.23
	8.12	*4.50*	*3.17*		*7.26* *7.16*
					4H 7.27
					7.24
Arg36	8.24	4.25	1.81	1.65	γCH$_2$ 1.53; δCH$_2$ 3.15
	8.06	*4.12*	*1.89*	*1.78*	*1.64* *3.19*
					δNH 7.14
					7.14
Gly37	7.83	3.84			
	8.14	*3.89*			
His38	8.42	4.69	3.25	3.14	2H 8.61; 4H 7.26
	8.16	*4.65*	*3.33*	*3.21*	*8.68* *7.32*
Met39	8.44	4.47	2.04	1.96	γCH$_2$ 2.49 2.49; SCH$_3$ 2.01
	8.04	*4.49*	*2.08*	*2.02*	*2.56* *2.50* *2.05*
Ala40	8.39	4.29	1.31		
	8.01	*4.23*	*1.39*		
Arg41	8.31	4.29	1.81	1.76	γCH$_2$ 1.62; δCH$_2$ 3.18
	7.98	*4.31*	*1.94*	*1.80*	*1.67* *3.22*
					δNH 7.19
					7.13
Lys42	8.40	4.29	1.81	1.70	γCH$_2$ 1.43; δCH$_2$ 1.76
	8.05	*4.31*	*1.89*	*1.69*	*1.46* *1.77*
					εCH$_2$ 2.99; εNH$_3^+$ 7.51
					3.03 *7.44*
Lys43	8.04	4.13	1.77	1.68	γCH$_2$ 1.39; δCH$_2$ 1.72
	7.82	*4.20*	*1.87*	*1.67*	*1.41* *1.74*
					εCH$_2$ 22.99; εNH$_3^{22}$ 7.51
					3.00 *7.42*

Top, 90% H_2O/10% D_2O; bottom (in italic), 55 mM SDS-d_{25}.

K42 exhibit a larger decrease in exchange rate in micellar solution. The three- to four-residue separation between these slowly exchanging amide protons is suggestive of a helical structure and preferential orientation for $NG_{(28-43)}$ in association with SDS micelle.

Deviations from the reference random coil values for the backbone NH chemical shifts of $NG_{(28-43)}$ and $[A^{35}]NG_{(28-43)}$ in water and in SDS solutions are presented in Fig. 7 (Bundi and Wüthrich, 1979; Wishart and Sykes, 1994; Merutka et al., 1995). An upfield shift of the NH chemical shift has been proposed to correlate with helix formation (Wishart et al., 1991). Scattered upfield or downfield shift is observed for the data of $NG_{(28-43)}$ displayed in Fig. 7 *A* in aqueous solution, whereas the chemical shift deviation is consistently upfield in SDS micelle solution, consistent with helix formation of the parent peptide in association with the SDS micelle. For the results of $[A^{35}]NG_{(28-43)}$ shown in Fig. 7 *B*, the degree of upfield shift is smaller than the parent peptide; some amide protons even exhibit a small downfield shift in the SDS solution. The data are consistent with a greater tendency toward helix formation by $NG_{(28-43)}$.

Fig. 8 *A* shows the ^{13}C spectra of SDS aliphatic chain in the absence of both peptide and spin label, and Fig. 8, *B* and *C*, display the corresponding data in the presence of $NG_{(28-43)}$ and in the presence of $NG_{(28-43)}$ plus the spin label, respectively. The linewidth and chemical shift of the peaks

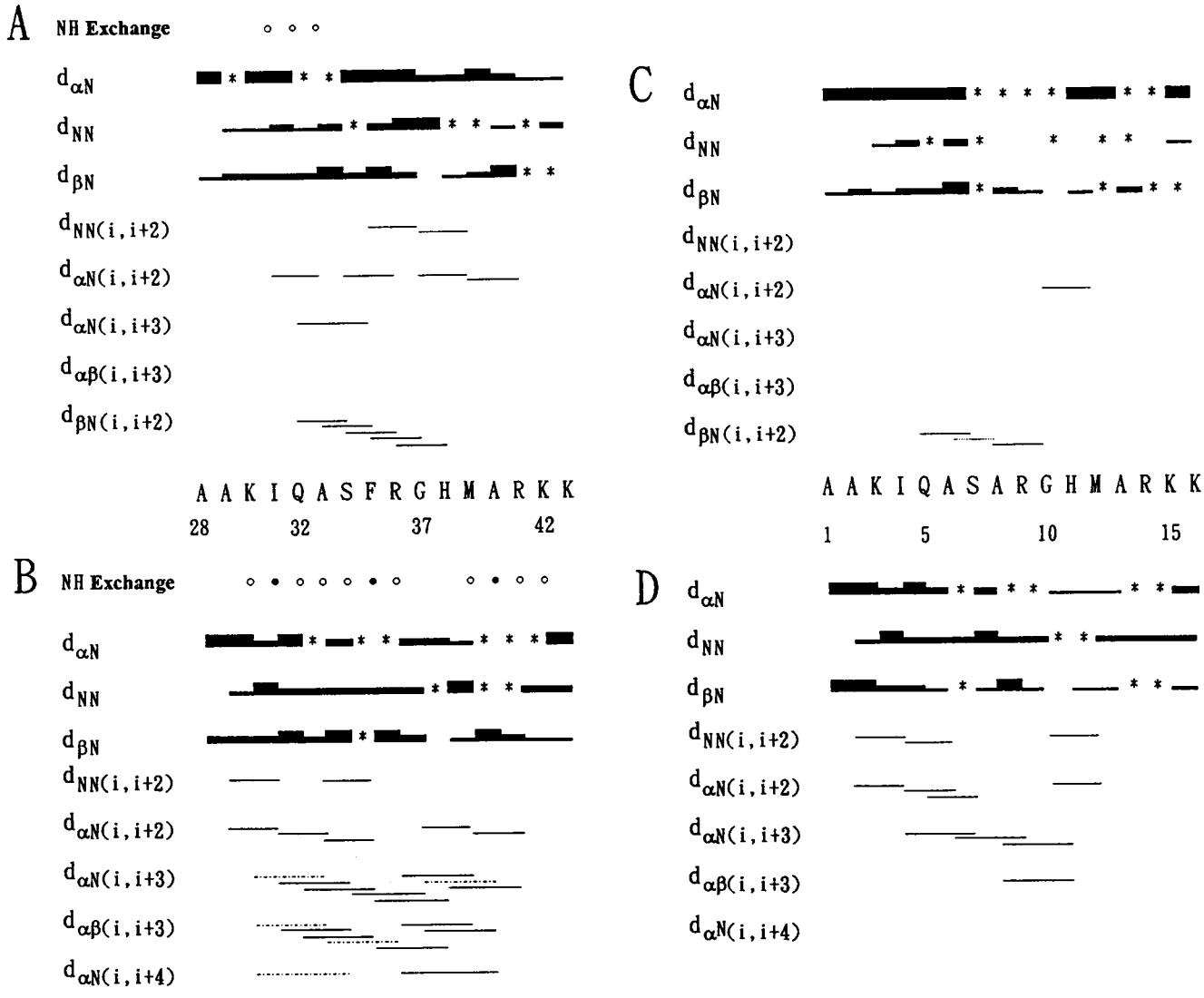

FIGURE 5 Summary of observed NOEs for $NG_{(28-43)}$ in water (*A*), in SDS micelles (*B*), and $[A^{35}]NG_{(28-43)}$ in water (*C*) and in SDS micelle solution (*D*). NOE intensities are indicated by the height of the bars. NOEs that are obscured, possibly because of overlapping resonances, are indicated by dashed lines or asterisks (*). The open circles shown on the top row of *A* represent the backbone NH resonance peaks that can be observed immediately after D_2O introduction into the lyophilized sample at 278 K; open and filled circles in *B* indicate the observable backbone NH resonance peaks after 20 min and 5 h, respectively, after introducing D_2O into a peptide/SDS mixture at 288 K.

are not changed by the addition of the peptide to the micelle, suggesting that the size of the micelle remains the same and perhaps that the peptide does not penetrate deep into the micellar interior. In contrast, a systematic decrease, from the tail of SDS, in the extent of linewidth broadening and chemical shift change (observed in Fig. 8 *C*), clearly shows that the spin label molecule penetrates to the center of the micelle. Fig. 8 also lends support to the notion of micelle formation for SDS at the concentrations used, consistent with the results shown in Fig. 1.

^1H NMR experiments were used to further characterize the association of $NG_{(28-43)}$ with SDS micelle. Fig. 9 illustrates the lineshape change of the parent peptide with SDS and the spin label. These results are summarized in Table 2 for the resonance peaks that can be at least partially resolved in one-dimensional spectra.

From a comparison of Fig. 9, *A* and *B*, it is can be seen that the effect is larger for residues I31, F35, and H38. For example, line broadening is more prominent for side-chain protons of I31, F35, and M39 and for the backbone amide protons of I31, Q32, and F35. In particular, the aromatic protons of F35 and γ-methyl protons of M39 shown in Fig. 9 *C* exhibit a larger broadening effect, suggesting a specific interaction with the spin label and thus with the SDS micelle. In contrast, the effect of 12-SASL is smaller for A33, G37, A40, and R41. It is of interest to note that the γ-methyl protons of I31 are broadened more than δ-methyl protons, indicating a preferential orientation of I31 side chain with

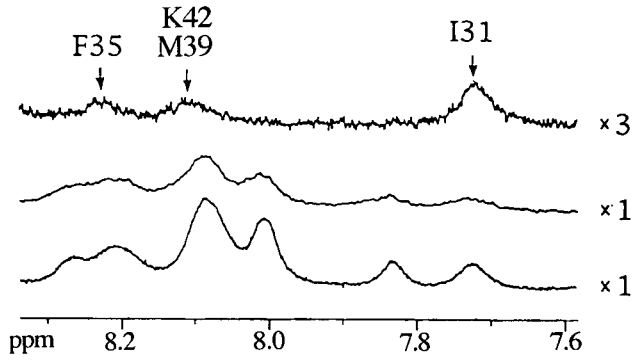

FIGURE 6 Low-field region ^{1}H spectrum of $NG_{(28-43)}$ at 288 K in SDS solution immediately (*bottom*), 20 min (*middle*), and 5 h (*top*) after introducing D_2O into the lyophilized peptide sample.

respect to the micelle. Moreover, the degeneracy of the two Q32 γH resoance peaks due to rotation of the side chain along C_β and C_γ in aqueous solution is lifted by restriction

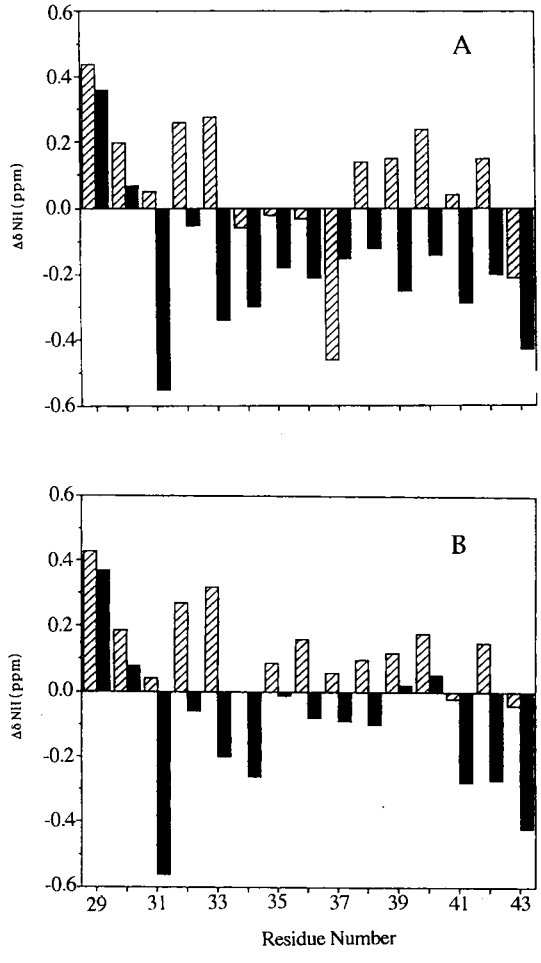

FIGURE 7 Plot of deviation of the chemical shifts of amide protons from random coil values, Δ(δNH), against residue number for $NG_{(28-43)}$ (*A*) and $[A^{35}]NG_{(28-43)}$ (*B*) in aqueous solution (*hatched bars*) and in SDS solution (*solid bars*). Negative chemical shift differences indicate upfield shift.

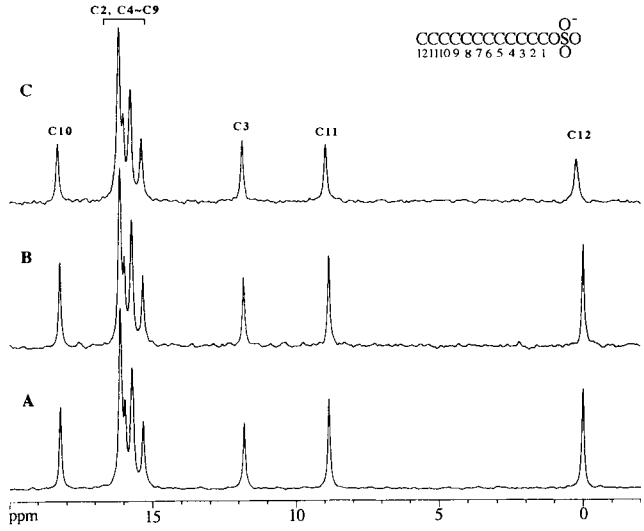

FIGURE 8 Natural abundance ^{13}C NMR spectra at 298 K of (*A*) 280 mM SDS, (*B*) 1.6 mM $NG_{(28-43)}$ in 280 mM SDS, and (*C*) 1.6 mM NG in 280 mM SDS with 4.4 mM 12-SASL. Linewidth broadening is most evident for ^{13}C at position 12 and decreases systematically toward the sulfate headgroup, suggesting that 12-SASL penetrates deeply into the SDS micelle.

on the rotation of the side chain resulting from its interaction with SDS micelle. Similarly, the resonance peaks of guanidinyl protons of R36 and R41 are split in the presence of SDS micelles. It is striking that a linewidth narrowing by 2.0 Hz (from 10 to 8 Hz) is observed for the side-chain amide protons of Q32 on interacting with SDS micelle. This can be explained by the fact that the amide proton resonance peaks are broadened because of exchange of protons on the side-chain amide group with those from the solvent in the SDS-free solution (Ernst et al., 1987); this proton exchange is slowed down by the hydrogen bond formed between the side chain of Q32 and SDS headgroups. All of these observations argue for the interaction of $NG_{(28-43)}$ peptide with SDS micelles and suggest formation of a helix with its preferential orientation.

Additional evidence for a helical $NG_{(28-43)}$ interacting with the SDS micelle is obtained from ^{1}H TOCSY experiments that exhibit the effect of the spin label on the $NG_{(28-43)}$:SDS micelle complex. A comparison of Fig. 10, *A* and *B*, reveals several linewidth broadening. Specifically, broadening effect by the spin label is more prominent for residues I31, Q32, F35, and M39, concurring with one-dimensional results shown in Fig. 9. These ^{1}H NMR results are summed up in the bottom portion of Table 2 for those residues that are resolvable in one-dimensional ^{1}H spectrum. It is seen that the periodicity of larger broadening apparently matches with an α-helical structure for the peptide associating with SDS micelle. In general, the broadening effect is smaller in the C-terminal than in the N-terminal portion of the peptide. Thus the effect on R41 or K42 is smaller than that on K30. Furthermore, by far the smallest broadening effect by the spin label is found in K43, dem-

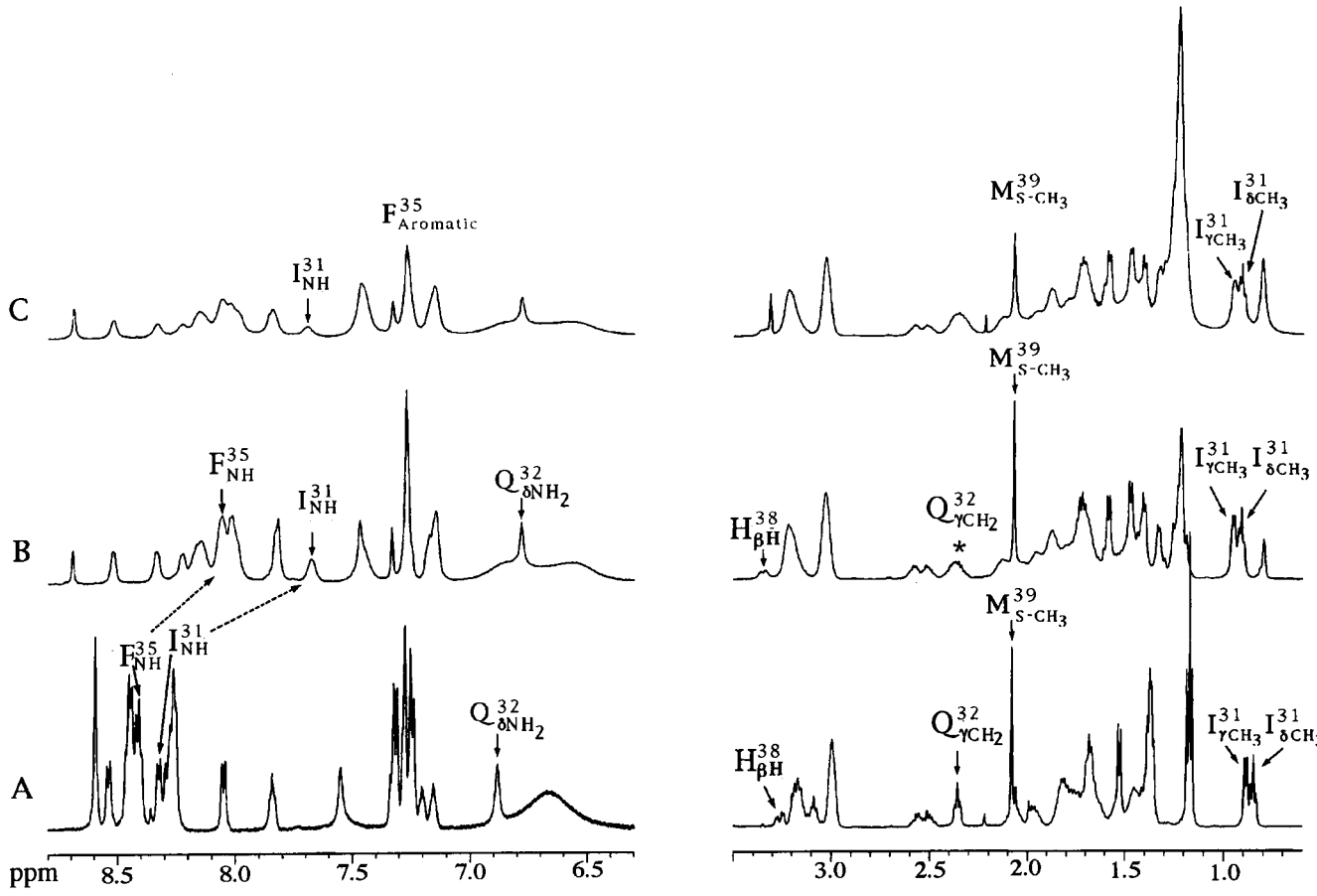

FIGURE 9 ^{1}H NMR spectra for (*A*) 2.2 mM $NG_{(28-43)}$ in aqueous solution, (*B*) 2.2 mM $NG_{(28-43)}$ in 55 mM SDS-d_{25}, and (*C*) 3 mM $NG_{(28-43)}$ in 124 mM SDS-d_{25} with 1.2 mM 12-SASL. A Lorentzian-to-Gaussian window function with line broadening of −0.3 Hz was applied to spectra *A* and *B* to show the fine splitting of γCH_2 of Q32 in SDS micellar solution, whereas 0.3-Hz linebroadening was applied to *C*. Labeled peaks indicate significant line broadening due to SDS and 12-SASL; the peak marked with an asterisk (*) denotes splitting of resonances in the presence of SDS micelles. In comparing *A* and *B*, note the linewidth narrowing and the apparent splitting for resonance peaks of the guanidinyl protons of arginine residues and side-chain amide proton of the glutamine residue. Dotted arrows between *A* and *B* indicate large upfield chemical shift for the amide protons of I31 and F35 of $NG_{(28-43)}$ upon introduction of SDS micelles.

onstrating the differential lineshape change caused by the spin label. This indicates that the C-terminal hydrophilic segment is not in contact with the micellar interior (see below and Fig. 15).

Both neurogranin and PKC are extrinsic membrane proteins because of lack of long stretches of the hydrophobic amino acid sequence. The linewidth of backbone amide proton resonances is calculated to be greater than 20 Hz for a helical peptide embedded in the interior of SDS micelles (Chang and Chien, unpublished result); however, the measured linewidth is less than 10 Hz. The linewidth data thus support the notion that $NG_{(28-43)}$ is associated extrinsically with SDS micelles.

Fig. 11 presents far UV-CD spectra of $NG_{(28-43)}$ peptide in solution containing SDS micelles, as well as vesicles formed by PS, PC, and PS/DAG phospholipids. The data indicate that more helix is induced, and hence there is a stronger peptide/micelle interaction, for micelles and vesicles containing negatively charged headgroups. The results indicate electrostatic contribution to the interaction between the cationic $NG_{(28-43)}$ and micelles or between the peptide and vesicles. It is of interest to note that the helix content is higher for the substrate peptide in PS/DAG vesicular solution than in PS vesicular and in SDS micellar solutions. Because helical structure was induced for PKC substrate $NG_{(28-43)}$ in solution containing PS/DAG, which stimulates PKC, a helix is likely the active form for the PKC substrate peptides or proteins. The induction of the $NG_{(28-43)}$ into a helical form by association with PS-containing vesicles may be biologically significant, because a model was recently proposed (Dong et al., 1995) in which the PKC and its substrate were thought to be brought together in close proximity because of their common affinity for PS.

Fig. 12 shows the CD spectra of $NG_{(28-43)}$ and $[A^{35}]NG_{(28-43)}$ in water as well as in SDS micelle solution. The data indicate that both peptide analogs exist predominantly in random form in aqueous solution, but significant helical form can be induced in the presence of SDS micelles

TABLE 2 Linewidth difference between $NG_{(28-43)}$ NMR signals in water and SDS and linewidth difference between $NG_{(28-43)}$ NMR signals in SDS in the absence and presence of spin-labeled 12-doxyl stearic acid methyl ester

Residue	NH	αH	βH	Others
Ala28			0.6	
Ala29	1.3		2.1	
Lys30	1.9			
	4.2			*εCH$_2$0*
Ile31	4.5	1.6		γCH$_2$ 2.7; γCH$_3$ 1.6; δCH$_3$ 1.1
	8.9			*γCH$_3$ >9.0; δCH$_3$ 2.2*
Gln32	1.9	2.0	δNH$_2$ 2.0	
	>5.0			
Ala33			2.2	
Phe35	4.8			2,6H 2.8; 3,5H 2.6
				2,6,5H 5.7
Arg36				*δCH$_2$ 1.3*
His38			>4.0	4H 2.3
			4.0	*4H 3.5; 2H 2.0*
Met39			2.1	SCH$_3$ 1.0
			2.9	*SCH$_3$ 4.8*
Ala40			2.1	
Arg41				*δCH$_2$ 1.3*
Lys42				*εCH$_2$ 0; δCH$_2$ 1.9*
Lys43				*εCH$_2$ 0; δCH$_2$ 1.9*

Top, Signals in water and SDS; bottom (italic), signals in SDS in the absence and presence of spin-labeled 12-doxyl stearic acid methyl ester.

(Yang et al., 1986). The helical content in SDS solution is calculated to be, respectively, 18% and 12% for $NG_{(28-43)}$ and $[A^{35}]NG_{(28-43)}$, with 50% more helix content for the parent peptide. This indicates that the membrane-bound peptides are in dynamic equilibrium with those in bulk solution. The higher induced helix content for $NG_{(28-43)}$ is in qualitative agreement with NOE data.

It should be emphasized that, for $NG_{(28-43)}$, the helical conformer exists only when the peptide is in association with the micelle. In fast exchange with the free state on the NMR time scale, the bound state accounts for, according to

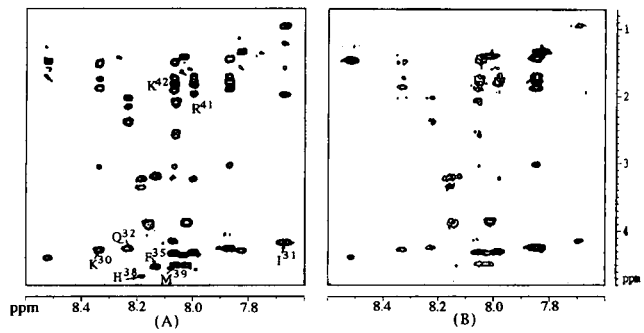

FIGURE 10 Side-chain proton-amide proton region of TOCSY spectra of 3 mM $NG_{(28-43)}$ in 124 mM SDS micelles in the absence (*A*) and presence (*B*) of 1.2 mM 12-SASL. Residues (K30, I31, Q32, F35, H38, and M39) that are broadened more extensively by the presence of 12-SASL are labeled. Cross-peaks from both R41 and K42 exhibit less broadening by 12-SASL, suggesting a weaker interaction of the C-terminal region of $NG_{(28-43)}$ with the micelle.

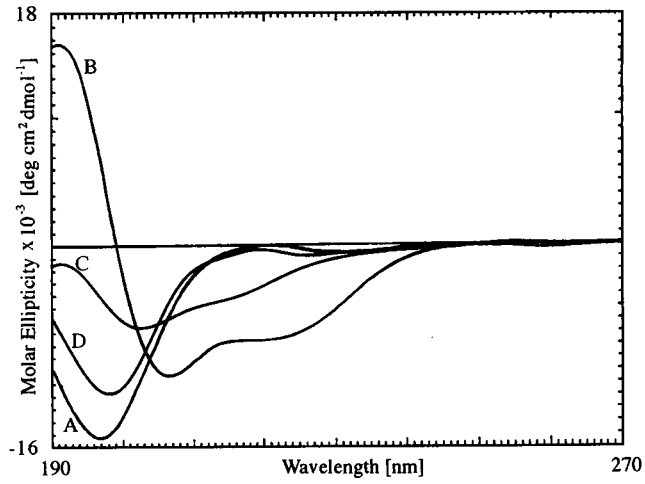

FIGURE 11 Circular dichroism spectra of $NG_{(28-43)}$ in TFE and various micellar solutions at 298 K and at pH 7 in (*A*) water; (*B*) 100% TFE; (*C*) 2 mM PC; (*D*) 2 mM PS; (*E*) 57 μM PS/3.5 μM DAG. In *C* and *D*, 20 μM NG(28–43) and, in *E*, 2.8 μM $NG_{(28-43)}$ was used.

the CD result, no more than 18% of total population. Because the ^{1}H-^{1}H NOE interaction is proportional to the inverse of the sixth power of the interproton distance, the folded structure is far more weighted than the unstructured conformers, so that the NOE pattern characteristic of helix can be observed, despite the smaller population for the bound state. This is a demonstration of transferred NOE (Forsén and Hoffman, 1963); in other words, the NOE information is transferred from the folded, bound state to the free state of the substrate.

In Fig. 13 is displayed the stereo drawing of the superposition of 20 structures calculated with distance geometry and dynamic simulated annealing, using constraints derived

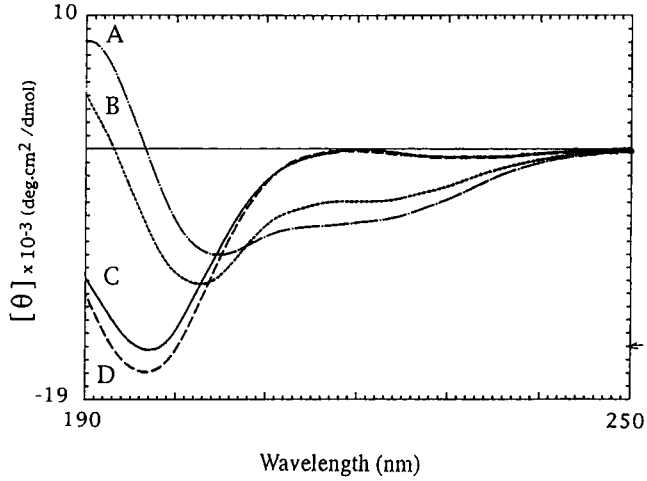

FIGURE 12 Circular dichroism spectra of $NG_{(28-43)}$ and $[A^{35}]NG_{(28-43)}$ in aqueous solution and in SDS micelles at 298 K and pH 7. Traces *A* and *B* represent the CD spectra of $NG_{(28-43)}$ and $[A^{35}]NG_{(28-43)}$ in 25 mM SDS. Traces *C* and *D* are the CD spectra of $NG_{(28-43)}$ and $[A^{35}]NG_{(28-43)}$ in aqueous solution, respectively.

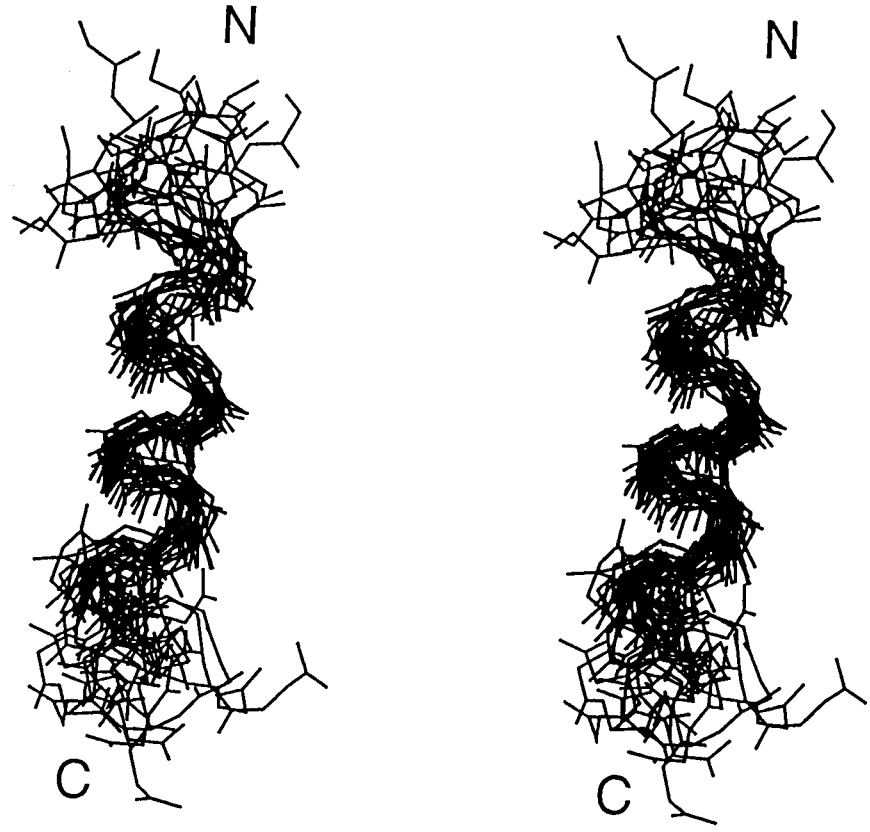

FIGURE 13 Stereo view of the overlayed 20 final simulated annealing structures of $NG_{(28-43)}$ calculated from the distance geometry/simulated annealing protocol using constraints derived from NMR experiments in the SDS micelle solution.

from NOE data of $NG_{(28-43)}$ in the SDS micelle solution. The root mean square deviation for the backbone atoms of $NG_{(28-43)}$ is 2.03 Å, and that for the backbone atoms of residues I31-A40 is 1.37 Å. A well-defined helical structure is visible in the region I31-A40.

A helical wheel representation for NG(28–43) is illustrated in Fig. 14, with the hydrophobic residues highlighted by asterisks. On the hydrophobicity scale, histidine residue is usually placed near serine as a protonated form (Kyte and Doolittle, 1982); however, it is likely to exist in neutral form in a less polar environment, such as membrane in which its hydrophobicity would be expected to be close to that of tryptophan (Garnier and Robson, 1990). Therefore, H38 may be part of the hydrophobic face of a helix. Hydrophobic forces have been reported to contribute to the helix formation of amphipathic peptides in the membrane or more hydrophobic environments (Thornton and Gorenstein, 1994; Bruch and Hoyt, 1992; Karslake et al., 1990). Fig. 15 depicts the interaction of $NG_{(28-43)}$ helix with the SDS micelle. The side chains of I31, Q32, F35, H38, and M39 are shown schematically to interact with SDS. In particular, the picture is consistent with the linewidth broadening data and splitting of the Q32 βH peak in SDS micelle solution. In support of the model, particularly with regard to the orientation of the peptide, the most significant reduction in the proton-deuterium exchange rate of the backbone amide protons in SDS micelle solution relative to that in aqueous solution can be found for residues I31, F35, M39, and K42 (Figs. 5 and 6). The C-terminus of $NG_{(28-43)}$ is not in the helical form, but participates in the ionic bonds with sulfate groups of SDS micelle, so that backbone amide protons of R41 and K42 exchange sufficiently slowly to be observed. That a weaker interaction exists between the C-terminal region and the micelle is in agreement with the linebroadening results from the paramagnetic probe (Fig. 10).

As suggested by the spin label probe experiments and the data shown in Table 2, a specific interaction is likely to exist between the nonpolar side chain of F35 and the membrane interior, so that the parent peptide would have higher affinity for the membrane than would its A35 analog. This specific interaction may also help orient the peptide in its approach to the active site of membrane-bound PKC. There may also be a specific interaction between F35 of the parent peptide or protein substrate and PKC (Knighton et al., 1991). (In this case, conformation of the substrate at the phosphorylation site would be changed, particularly if the interaction does not occur in the interior or the immediate vicinity of membrane.) Moreover, from both CD and NOE results, the helical content is lower for the A35 analog, which would require larger free energy of activation for the phosphorylation to proceed because of larger entropy loss in going from the reactant to its transition state. These factors would contribute in part to the dramatic reduction in the

catalytic efficiency of PKC for the A35 mutant of $NG_{(28-43)}$ in the presence of lipid membrane (Chen et al., 1993).

Based on data from the present study and previous reports on the properties of phosphorylation kinetics, the following model is proposed (cf. Fig. 15). PKC substrates are attracted to the surface of the phospholipid bilayer by long-range electrostatic force, as suggested by the induction of $NG_{(28-43)}$ in SDS micellar and in PS/DAG vesicular solutions (Fig. 11). The substrate then undergoes reorientation due to specific interaction with the membrane and may diffuse on the surface of the membrane. Alternatively, binding of the substrate to membrane may induce PKC to translocate to the membrane (Bruins and Epand, 1995), leading to substrate phosphorylation. This model apparently accounts, in part, for the contribution of the negatively charged phosphatidyl serine to the phosphorylation rate and the essential role played by the nonpolar amino acid immediately C-terminal to the phosphorylation site. The importance of rate of encounter has been predicated by Houbre et al., who pointed out that the delivery of substrate to the reactive site was a key event in PKC phosphorylation (Houbre et al., 1991).

The use of SDS micelle as model membrane probably emphasizes electrostatic interaction over other forces, such as hydrogen bond and hydrophobic effect. Despite this limitation, evidence from NMR experiments was presented for the specific hydrophobic interaction between the micelle and F35 C-terminal to the phosphorylation site. Other nonpolar amino acid residues in $NG_{(28-43)}$ are not required for phosphorylation by PKC, but results on the lineshape modification in NMR experiments suggest that these residues might provide supplementary stabilization on the orientation of the substrate bound to membrane. The role of the nonpolar moieties of the PKC substrate can perhaps be exemplified by the membrane anchoring of the myristoyl chain on the MARCKS (myristoylated alanine-rich protein kinase C substrate; Kim et al., 1994; Buss et al., 1986). The model proposed here suggests that it would stabilize substrate-membrane interaction and thereby may enhance the phosphorylation efficiency, to employ amino acid residues with long nonpolar side chains at positions that make helical

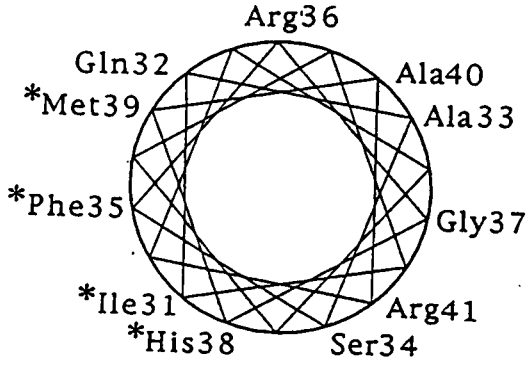

FIGURE 14 Helical wheel representation of $NG_{(28-43)}$. Hydrophobic residues lying on one face of the helix are marked by asterisks (*).

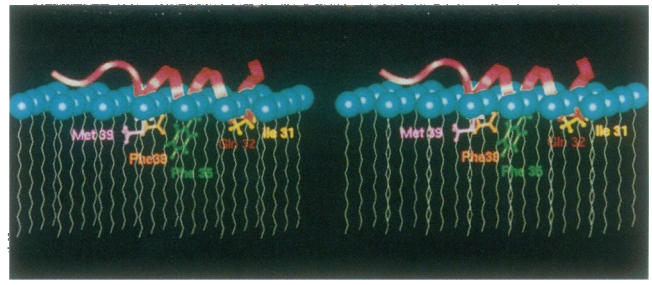

FIGURE 15 Schematic drawing illustrating the interaction of NG(28–43) peptide with the SDS micelle. The side chains of I31, Q32, F35, H38, and M39 are marked to emphasize specific interactions between them and the micelle.

register, similar to the neurogranin and neuromodulin phosphorylation domain.

The present detailed study on the nature of interaction between a PKC substrate and the model membrane represents a first step toward understanding, on the molecular level, of the ternary complex formed between these two components and PKC. Dealing with the interaction between a single substrate peptide and single negatively charged micelle (or vesicle) only, the working model does not address the aggregation brought about by interactions between some cationic polypeptides and PS/DAG/Ca^{2+}/detergent micelles, as reported by Mahoney and Huang (1995). Nor are the specific interactions considered between the substrate and other components on the cell membrane bilayer, e.g., PE (phosphotidylethanolamine), PI (phosphotidylinositol), and SM (sphingomyelin). For a complete description, the complex interactions between the enzyme PKC, its substrate, the cofactors, and the membrane must be determined (Kaibuchi et al., 1981).

The authors thank Ms. Shu-Fang Cheng for acquiring CD spectra in PS-containing solution, as well as Drs. Shu-Hua Chien and Jang-Cheng Ho for obtaining EPR spectra.

This work was supported by Academia Sinica and the National Science Council of the Republic of China (NSC-84-2113-M-001-007).

REFERENCES

Aderem, A. 1992. Signal transduction and the actin cytoskeleton: the roles of MARCKS and profilin. *Trends Biochem. Sci.* 17:438–443.

Baudier, J., C. Bronner, D. Kligman, and R. D. Cole. 1989. Protein kinase C substrates from bovine brain. Purification and chararcterization of neuron-specific calmodulin-binding protein. *J. Biol. Chem.* 264: 1824–1828.

Baudier, J., J. Deloume, A. V. Dorsselaer, D. Black, and H. W. D. Mattes. 1991. Purification and characterization of a brain-specific protein kinase C substrate neurogranin (p17): identification of a consensus amino acid sequence between neurogranin and neuromodulin (GAP 43) that corresponds to the protein kinase C phosphorylation site and the calmodulin-binding domain. *J. Biol. Chem.* 266:229–237.

Bax, A., and D. G. Davis. 1985. MLEV-17-based two-dimensional homonuclear magnetization transfer spectroscopy. *J. Magn. Reson.* 65: 355–360.

Bazzi, M. D., and G. L. Nelsestuen. 1987. Role of substrate in determining the phosphlipid specificity of protein kinase C activation. *Biochemistry.* 26:5002–5008.

Bodenhausen, G., H. Kogler, and R. R. Ernst. 1984. Selection of coherence-transfer pathways in NMR pulse experiments. *J. Magn. Reson.* 58:370–388.

Braunschweiler, L., and R. R. Ernst. 1983. Coherence transfer by isotropic mixing: application to proton correlation spectroscopy. *J. Magn. Reson.* 53:521–528.

Brown, L. R., C. Bösch, and K. Wüthrich. 1981. Location and orientation relative to the micelle surface for glucagon in mixed micelles with dodecylphosphocholine. *Biochim. Biophys. Acta.* 632:296–312.

Bruch, M. D., and D. W. Hoyt. 1992. Conformational analysis of a mitochondrial presequence derived from the F_1-ATPase β-subunit by CD and NMR spectroscopy. *Biochim. Biophys. Acta.* 1159:81–93.

Bruins, R. H., and R. M. Epand. 1995. Substrate-induced translocation of PKC-α to the membrane. *Arch. Biochem. Biophys.* 324:216–222.

Bundi, A., and K. Wüthrich. 1979. ^{1}H-NMR parameters of the common amino acid residues measureed in aqueous solution of the linear tetrapeptides H-Gly-Gly-X-L-Ala-OH. *Biopolymers.* 18:285–298.

Buss, J. E., M. P. Kemps, K. Gould, and B. M. Sefton. 1986. The absence of myristic acid decreases membrane binding of p60src but does not affect tyrosine protein kinase activtity. *J. Virol.* 58:468–474.

Cannon, B., C. F. Polnaszek, K. W. Butler, L. E. G. Eriksson, and I. C. P. Smith. 1975. The fluidity and organization of mitochondrial membrane lipids of the brown adipose tissue of cold-adapted rats and hamsters as determined by nitroxide spin probes. *Arch. Biochem. Biophys.* 167: 505–518.

Chen, S. J., E. Klann, M. C. Gower, C. M. Powell, J. S. Sessoms, and J. D. Sweatt. 1993. Studies with synthetic peptide substrates derived from the neuronal protein neurogranin reveal structural determinants of potency and selectivity for protein kinase C. *Biochemistry.* 32:1032–1039.

Davis, R. J., G. L. Johnson, D. J. Kelleher, J. K. Anderson, J. E. Mole, and M. P. Czech. 1986. Identification of serine 24 as the unique site on the transferrin receptor phosphorylated by protein kinase C. *J. Biol. Chem.* 261:9034–9041.

Dekker, L. V., P. N. E. De Graan, D. H. G. Versteeg, A. B. Oestreicher, and W. H. Gipsin. 1989. Phosphorylation of B-50 (GAP43) is correlated with neurotransmitter release in rat hippocampal slices. *J. Neurochem.* 52:24–30.

Devaux, P. F. 1992. Protein involvement in transmembrane lipid asymmetry. *Annu. Rev. Biophys. Biomol. Struct.* 21:417–439.

Dong, L., C. Chapline, B. Mosseau, L. Fowler, K. Ramsay, J. L. Stevens, and S. Jaken. 1995. 35H, a sequence isolated as a protein kinase C binding protein, is a novel member of the adducin family. *J. Biol. Chem.* 270:25534–25540.

Edashige, K., T. Utsumi, E. F. Sato, M. Kasai, and K. Utsumi. 1992. Requirement of protein association with membrane for phosphorylation by protein kinase C. *Arch. Biochem. Biophys.* 296:296–301.

Englander, J. J., D. B. Calhounn, and S. W. Englander. 1979. Heat-stable enterotoxin of *Escherichia coli*: in vitro effects on guanylate cyclase activity, cyclic GMP concentration, and ion transport in small intestine. *Proc. Natl. Acad. Sci. USA.* 75:2800–2804.

Ernst, R. R., G. Bodenhausen, and A. Wokaun. 1987. Principles of Nuclear Magnetic Resonance in One and Two Dimensions. Oxford University Press, New York. 214–215.

Forsén, S., and R. A. Hoffman. 1963. Study of moderately rapid chemical exchange reactions by means of nuclear magnetic double resonance. *J. Chem. Phys.* 39:2892–2901.

Garnier, J., and B. Robson. 1990. The GOR method for predicting secondary structures in proteins. *In* Prediction of Protein Structure and the Principles of Protein Conformation. Plenum Press, New York.

Gianotti, C., M. G. Nunzi, W. H. Gispen, and R. Corradetti. 1992. Phosphorylation of the presynaptic protein B-50 (GAP-43) is increased during electrically induced long-term potentiation. *Neuron.* 8:843–848.

Houbre, D., G. Duprotail, J. C. Deloulme, and J. Baudier. 1991. The interactions of the brain-specific calmodulin-binding protein kinase C substrate, neuromodulin (GAP 43), with membrane phospholipids. *J. Biol. Chem.* 266:7121–7131.

Huang, F. L., Y. Yoshida, N. Yakabayashi, and K. P. Huang. 1987. Differential distribution of protein kinase C isozymes in the various regions of the brain. *J. Biol. Chem.* 262:15714–15720.

Huang, K.-P. 1989. The mechanism of protein kinase C activation. *Trends Neurosci.* 12:425–432.

Huang, K.-P., H. Nakabayashi, and F. L. Huang. 1986. Isozymic forms of rat brain Ca^{+2}-activated and phospholipid-dependent protein kinase C activation. *Proc. Natl. Acad. Sci. USA.* 83:8535–8539.

Hurd, R. E. 1990. Gradient-enhanced spectroscopy. *J. Magn. Reson.* 87: 422–428.

Jackman, L. M., and S. Sternhell. 1969. Applications of Nuclear Magnetic Resonance Spectroscopy in Organic Chemistry, 2nd Ed. Pergamon Press, Oxford. 95.

Jeener, J., B. H. Meier, P. Bachmann, and R. R. Ernst. 1979. Investigation of exchange process by two-dimensional NMR spectroscopy. *J. Chem. Phys.* 71:4546–4553.

Kaibuchi, K., Y. Takai, and Y. Nishizuka. 1981. Cooperative roles of various membrane phospholipids in the activation of calcium-activated, phospholipid-dependent protein kinase. *J. Biol. Chem.* 256:7146–7149.

Karplus, M. 1959. Contact electron-spin coupling of nuclear magnetic moments. *J. Chem. Phys.* 30:11–15.

Karslake, C., M. E. Piotto, Y. M. Pak, H. Weiner, and D. G. Gorenstein. 1990. 2D NMR and structural model for a mitochondrial signal peptide bound to a micelle. *Biochemistry.* 29:9872–9878.

Kim, J., T. Shishido, X. Jiang, A. Aderem, and S. McLaughlin. 1994. Phosphorylation, high ionic strength, and calmodulin reverse the binding of MARCKS to phospholipid vesicles. *J. Biol. Chem.* 269: 28214–28219.

Klann, E., S. J. Chen, and J. D. Sweatt. 1992. Increased phosphorylation of a 17-kDa protein kinase C substrate (P17) in long-term potentiation. *J. Neurochem.* 58:1576–1579.

Knighton, D. R., J. Zheng, L. F. Ten Eyck, N. H. Xuong, S. S. Taylor, and J. M. Sowadski. 1991. Structure of a peptide inhibitor bound to the catalytic subunit of cyclic adenosine monophosphate-dependent protein kinase. *Science.* 253:414–420.

Koide, H., K. Ogita, U. Kikkawa, and Y. Nishizuka. 1992. Isolation and characterization of the ϵ-subspecies of protein kinase C from rat brain. *Proc. Natl. Acad. Sci. USA.* 89:1149–1153.

Kragh-Hansen, U., and T. Riisom. 1976. Complexes of aliphatic sulfates and human-serum albumin studied by ^{13}C nuclear magnetic resonance spectroscopy. *Eur. J. Biochem.* 70:15–23.

Kumar, A., R. R. Ernst, and K. Wüthrich. 1980. A two-dimensional nuclear Overhauser enhancement (2D NOE) experiment for the elucidation of complete proton-proton cross-relaxation networks in biological macromolecules. *Biochem. Biophys. Res. Commun.* 95:1–5.

Kyte, J., and R. F. Doolittle. 1982. A simple method for displaying the hydropathic character of a protein. *J. Mol. Biol.* 157:105–132.

Macura, S., Y. Huang, D. Suter, and R. R. Ernst. 1981. Two-dimensional chemical exchange and cross-relaxation spectroscopy of coupled nuclear spins. *J. Magn. Reson.* 43:259–281.

Mahoney, C. W., and K.-P. Huang. 1995. Selective phosphorylation of cationic polypeptide aggregated with phosphotidylserine/diacylglycerol/Ca^{2+}/detergent mixed micelles by Ca^{2+}-independent but not Ca^{2+}-dependent protein kinase C isozymes. *Biochemistry.* 34:3446–3454.

Marion, D., and K. Wüthrich. 1983. Application of phase sensitive two-dimensional correlated spectrosocopy (COSY) for measurements of ^{1}H-^{1}H spin-spin coulping constants in proteins. *Biochem. Biophys. Res. Commun.* 113:967–974.

Meiri, K. F., M. Willard, and H. I. Johnson. 1988. Distribution and phosphoproteins of the growth-associated protein GAP-43 in regenerating sympathetic neurons in culture. *J. Neurosci.* 8:2571–2581.

Merutka, G., H. J. Dyson, and P. E. Wright. 1995. Random coil ^{1}H chemical shifts obtained as a function of temperature and trifluoroethanol concentration for the peptide series GGXGG. *J. Biomol. NMR.* 5:14–24.

Mysels, K., and L. H. Prinzen. 1959. Light scattering by some sulfate solutions. *J. Phys. Chem.* 63:1696–1700.

Nelson, R. B., D. I. Linden, C. Hyman, H. H. Pfenninger, and A. Routtenberg. 1989. The two major phosphoproteins in growth cones are probably identical to two protein kinase C substrates correlated with persistence of long-term potentiation. *J. Neurosci.* 9:381–389.

Nilges, M., G. M. Clore, and A. M. Gorenborn. 1988. Determination of three-dimensional structures of proteins from interproton distance data by hybrid distance geometry-dynamical simulated annealing calculations. *FEBS Lett.* 229:317–324.

Nishizuka, Y. 1988. The molecular heterogeneity of protein kinase C and its implications for cellular regulation. *Nature.* 334:661–665.

Oestreicher, A. B., J. J. H. Hens, A. Marquart, M. Merken, N. E. De Graan, H. Zwiers, and W. H. Gispen. 1994. Monoclonal antibody NM2 recognize the protein kinase C phosphorylation site in B-50 (GAP-43) and in neurogranin (BICKS). *J. Neurochem.* 62:881–889.

Ogita, K., S. I. Miyamoto, K. Yamaguchi, H. Koide, N. Fujisawa, U. Kikkawa, S. Sahara, Y. Fukami, and Y. Nishizuka. 1992. Isolation and characterization of δ-subspecies of protein kinase C from rat brain. *Proc. Natl. Acad. Sci. USA.* 89:1592–1596.

Pearson, R. B., and B. E. Kemp. 1991. Protein kinase phosphorylation site sequences and consensus specificity motifs: tabulations. *Methods Enzymol.* 200:62–81.

Piantini, U., O. W. Sörensen., G. Bodenhausen, G. Wagner, R. R. Ernst, and K. Wüthrich. 1982. Multiple quantum filters for elucidating NMR coupling networks. *J. Am. Chem. Soc.* 104:6800–6801.

Piotto, M., V. Saudek, and V. Sklenar. 1992. Gradient-tailored excitation for single-quantum NMR spectroscopy of aqueous solutions. *J. Biomol. NMR.* 2:661–665.

Ptitsyn, O. B., and A. V. Finkelstein. 1983. Theory of protein secondary structure and algorithm of its prediction. *Biopolymers.* 22:15–25.

Rance, M., O. W. Sörenson, G. Bodenhausen, G. Wagner, R. R. Ernst, and K. Wüthrich. 1983. Improved spectral resolution in COSY ^{1}H NMR spectra of proteins via double quantum filtering. *Biochem. Biophys. Res. Commun.* 117:479–485.

Redfield, A. G., and S. D. Kuntz. 1975. Quadrature fourier NMR detection: simple multiplex for dual detection and discussion. *J. Magn. Reson.* 19:250–254.

Represa, A., J. C. Deloulme, M. Sensenbrenner, Y. Ben-Ari, and J. Baudier. 1990. Neurogranin: immunocytochemical localization of brain-specific protein kinase C substrate. *J. Neurosci.* 10:3782–3792.

Richardson, J. S., and D. C. Richardson. 1989. Principles and patterns of protein conformation. *In* Prediction of Protein Structure and the Principles of Protein Conformation. G. D. Fasman, editor. Plenum Press, New York. 1–98.

Scholtz, J. M., H. Qian, E. J. York, J. M. Stewart, and R. L. Baldwin. 1991. Parameters of helix-coil transition theory for alanine-based peptides of varying chain lengths in water. *Biopolymers.* 31:1463–1470.

Shaka, A. J., and R. Freeman. 1983. Simplification of NMR spectra by filtration through multiple-quantum coherence. *J. Magn. Reson.* 51: 169–173.

Skene, J. H. P., and I. Virág. 1989. Posttranslational membrane attachment and dynamic fatty acylation of a neuronal growth cone protein, GAP-43. *J. Cell. Biol.* 108:613–624.

Stone, R. J., T. Buckman, P. L. Nordio, and H. M. McConnell. 1965. Spin label biomolecules. *Proc. Natl. Acad. Sci. USA.* 54:1010–1017.

Thornton, K., and D. G. Gorenstein. 1994. Structure of grucagon-like peptide (7-36) amide in a dodecylphosphocholine micelle as determined by 2D NMR. *Biochemistry.* 33:3532–3539.

Watson, J. B., E. F. Battenberg, K. K. Wong, F. E. Bloom, and J. G. Sutcliffe. 1990. Subtractive cDNA cloning of RC3, a rodent cortex-enriched mRNA encoding a novel 78 residue protein. *J. Neurosci. Res.* 26:397–408.

Wishart, D. S., and B. D. Sykes. 1994. Chemical shifts as a tool for structure determination. *Methods Enzymol.* 239:363–392.

Wishart, D. S., B. D. Sykes, and F. M. Richards. 1991. Relationship between nuclear magnetic resonance chemical shift and protein secondary structure. *J. Mol. Biol.* 222:311–333.

Wüthrich, K. 1986. NMR of Proteins and Nucleic Acids. Wiley, New York.

Yang, J. T., C. S. C. Wu, and H. M. Martinez. 1986. Calculation of protein conformation from circular dichroism. *Methods Enzymol.* 130:208–269.